GNHeII J1236+6215: A He II λ1640 emitting and potentially LyC leaking galaxy at $z = 2.9803$ unveiled through JWST & Keck observations

Chayan Mondal,[1,2] Kanak Saha,[2] Anshuman Borgohain,[2] Brent M. Smith,[3] Rogier A. Windhorst,[3] Naveen Reddy,[4] Chian-Chou Chen,[1] Keiichi Umetsu,[1] and Rolf A. Jansen[3]

[1]Academia Sinica Institute of Astronomy and Astrophysics (ASIAA), No. 1, Section 4, Roosevelt Road, Taipei 106319, Taiwan
[2]Inter-University Centre for Astronomy and Astrophysics, Ganeshkhind, Post Bag 4, Pune 411007, India
[3]School of Earth & Space Exploration, Arizona State University, Tempe, AZ 85287-1404, USA
[4]Department of Physics and Astronomy, University of California, Riverside, 900 University Avenue, Riverside, CA 92521, USA

Introduction

- Pop III stars contribute to ionize H or He^{+}
  - detection of high ionization emission lines (e.g., He II λ1640) can be used to infer their presence
- combined detection of HeII λ1640 and Lyα lines is a signature of hosting Pop III stellar populations (Tumlinson et al. 2001)

↔both recombination lines can be generated by astrophysical sources other than Pop III stars
  - the cooling of pristine metal-free gas
  - massive WR stars or AGN
  - slow but strong wind of low-metallicity very massive stars (VMS)
  - massive binary stars, winds driven by Supernova, and X-ray binaries in low metallicity environments

Data and Analysis

- GNHeII J1236+6215 (G1): He II λ1640 emitting LBG at z = 2.9803 ± 0.001
  - multi-band photometric and spectroscopic data from X-ray to radio wavelength
    - for spectroscopic analysis
      - obtain the *H* and *Ks* band MOSDEF spectra from the *MOSDEF data archive*
      - He II λ1640 line from Keck/LRIS spectrum
      - JWST NIRSpec spectra from *JADES data release*
    - for photometric analysis
      - HST WFC3 UVIS and ACS images and JWST NIRCam images (total 17 photometric bands
- SED fitting with CIGALE
  - for G1, constrain values from the emission line measurements
    - BC03 stellar population models (Bruzual & Charlot 2003) with a Chabrier IMF (Chabrier 2003)
    - exponential SFH added with a recent burst of varying strength
- spectrum (Figure4)
  - LRIS 1D spectrum
    - identify two rest-frame FUV emission lines (Lyα λ1215 and HeII λ1640) with S/N> 4
  - JWST NIRSpec spectrum
    - identify other emission lines than HeII λ1640

→derive line fluxes from the respective continuum-subtracted spectra(Table4)

Discussion

Properties of GNHeII J1236+6215(G1)

- UV absolute magnitude (M_{UV}) = −22.09 ± 0.02 mag
- interstellar reddening E(B−V) = 0.04 ± 0.12
- SFR from the rest-frame FUV, Hβ, Hα, and Paβ line fluxes are 9.8 ± 0.1, 7.6 ± 0.4, 7.5 ± 0.1, 6.40 ± 0.03 $M_{\odot}yr^{-1}$
  - agree well with the SED-derived value of 12.2 ± 2.0 $M_{\odot}yr^{-1}$
- [SII] BPT diagnostic (Figure5) to understand the ionized state of ISM

→ • G1 is in the region of star formation compared with the diagnostic relation
  - closely overlap with line ratios of low-z LyC leakers and HeII λ4686 emitting ionized metal-poor (IMP) galaxies
- S23: proxy to derive the nebular oxygen abundance in a galaxy

→gas-phase oxygen abundance of the galaxy : 12 + log(O/H) = 7.85 ± 0.22

⇨ G1 is a UV-luminous metal-poor star-forming galaxy with low dust content

Characteristics of the HeII λ1640 line (Figure6)

- G1 shows narrow FWHM (observed FWHM=573 ± 191 km s^{-1})
- G1 is luminous HeII emitters with HeII λ1640 line luminosity of 9.55 ± 1.95 × 10^{41} erg s^{-1}
- identify three more helium lines (HeI λ5875, HeII λ8236, HeI λ10830)
  - HeII λ8236 line has the same ionization potential as HeII λ1640
  - HeI λ10830 transition: strongest dependence on the electron density (Aver et al. 2015)

⇨reinforces the presence of an extreme ionizing source in G1

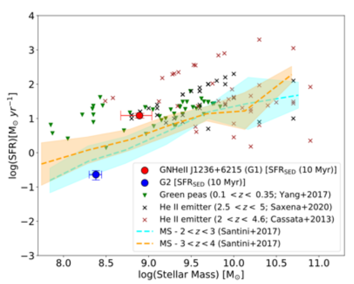

Figure 3. The derived SFR and stellar mass of G1 and G2 are shown by the red and blue markers, respectively. The main sequence (MS)

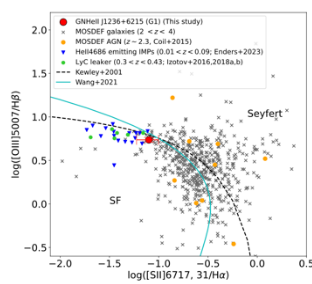

Figure 5. [SII] BPT diagram that shows the location of galaxy GNHeII J1236+6215 (red point) with respect to other populations. The

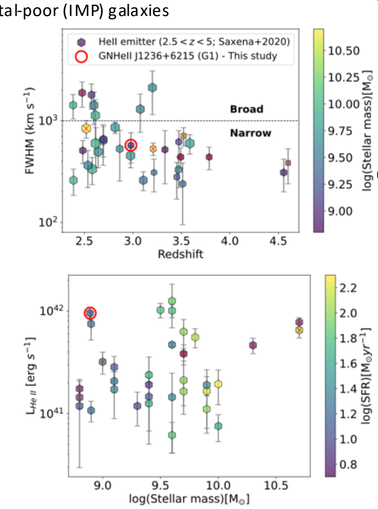

Figure 6. Properties of our identified He II λ1640 line is shown along with measurements of 33 He II emitters (hexagonal markers) reported by Saxena et al. (2020) between redshift ∼ 2.5 and 5. The

Discussion

Origin of narrow HeII λ1640 emission

- AGN or WR stars
  - narrow FWHM of the He II λ1640 line in G1

↔the expected line width from AGN or WR stars would be broader
  - narrow Balmer lines (FWHM ≲300 km s−1)
  - not distinctly identify higher-ionization emission lines (CIV λ1549, NV λ1240) in G1
  - non-detection of G1 in 2MS Chandra X-ray catalog
  - star-forming nature of ionization inferred from [SII] BPT diagnostic

⇨ He+ ionization in G1 is less likely due to AGNs or metal-rich WR stars
- infalling pristine gas
  - derived SFR and UV luminosity of G1 agree with this possibility
    - higher gas infall would increase star formation in the galaxy
    - detection of Lyα line in G1 supports the pristine gas-infalling case
- Pop III stars
  - gas-phase metallicity of G1 contradicts the presence of metal-free Pop III stars

↔Pop III stars can form in metal-enriched galaxies at z=6-7, using hydrodynamical simulation (Venditti et al. 2024)

⇨ • indicate that a population of metal-enriched stars contribute the identified O and S lines

↔a small number of newly formed Pop III stars can power He+ ionization
  - non-detection of strong C and N lines indicates that G1 could hold pockets of pristine gas to form Pop III stars
- metal-poor VMS
  - inclusion of VMSs can enhance the UV luminosity by 5-6 times from that of a normal SED (Schaerer et al. 2025)

⇨ high UV luminosity of G1 could indicate the existence of VMSs
  - observed UV continuum slope (β_{obs} = −2.18 ± 0.06) agrees well with models produced with VMSs

⇨possible that the He^{+} ionization in G1 is driven by metal-poor VMS formed during the ongoing burst

→Pop III diagnostic diagrams(Figure7): distinguish the contribution of Pop III stars from the others
  - HeII1640/Hα ratio of G1 falls within the range of ionization by Pop III stars (Katz et al. 2023)

↔[OIII] 5007/Hβ has a much higher value than what is expected from galaxies with only Pop III stars

⇨indicate that G1 could host small pockets of Pop III-like star formation along with normal populations

⇨ • HeII λ1640 emission in G1 is most likely powered either by pockets of Pop III stars or extremely metal-poor VMS
  - possibility of AGN or WR stars to drive He+ ionization in G1 is rather low

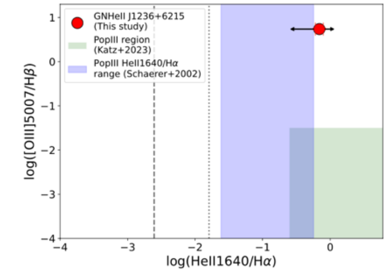

Figure 7. [OIII] 5007/Hβ vs He II 1640/Hα line ratio of GNHeII J1236+6215 (red point). The black arrow indicates the uncertainty

A potential LyC leaker

- detection of high ionization He II, [OIII], [SIII] lines in G1

⇨indicates that G1 produces enough ionizing photons to ionize H, leading to an ISM transparent to LyC photons
- find favorable ISM condition in G1 that can allow LyC photons to escape
  - high O32 and [SIII]/[SII], the presence of Balmer lines, and [SIII]9069,9532 lines of G1 indicates a higher ionized state of ISM
    - observed [SIII]/[SII] value infers a higher ionization potential (logU ≃ −3 - −2)
    - estimated upper limit of [OI]/[OIII] flux ratio = 0.013 is much smaller than O32

⇨supports density-bounded ionization and disfavors contribution from shock or AGN (Plat et al. 2019)
    - values of O32, metallicity, E(B−V), SFR surface density, and stellar mass of G1 fall within the regime of galaxies which host favorable ISM condition for leaking LyC photons (Figure 8)
    - G1 shows a compact morphology

⇨compact nature and high SFR surface density enhance the possibility of LyC leakage in G1 (Verhamme et al. 2017)
    - E(B−V) and observed β indicate a low dust extinction

⇨favor the escape of ionizing photons
    - the ionization potential of [SII] line is smaller than H

⇨low [SII]/Hα signifies a density-bounded optically thin HII region where the ionizing photons can escape efficiently

⇨G1 is a LyC leaker candidate at $z \sim 3$

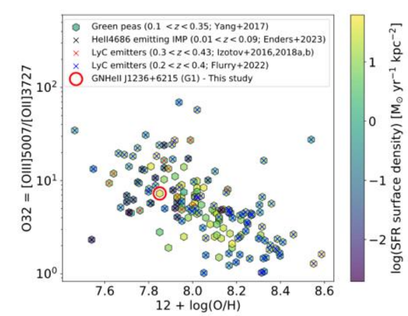

Figure 8. Gas-phase oxygen abundance 12 + log(O/H) and O32 ratio of the galaxy GNHeII J1236+6215 (marked with red circle)

Summary

- report the discovery of a low-mass metal-poor He II λ1640 emitting galaxy GNHeII J1236+6215 at z = 2.9803
- ionization by Pop III stars formed in small pockets of pristine gas or metal-poor VMSs formed during the ongoing burst could best explain narrow He II λ1640 line-width in G1

favor the escape of Lyman continuum photons from G1

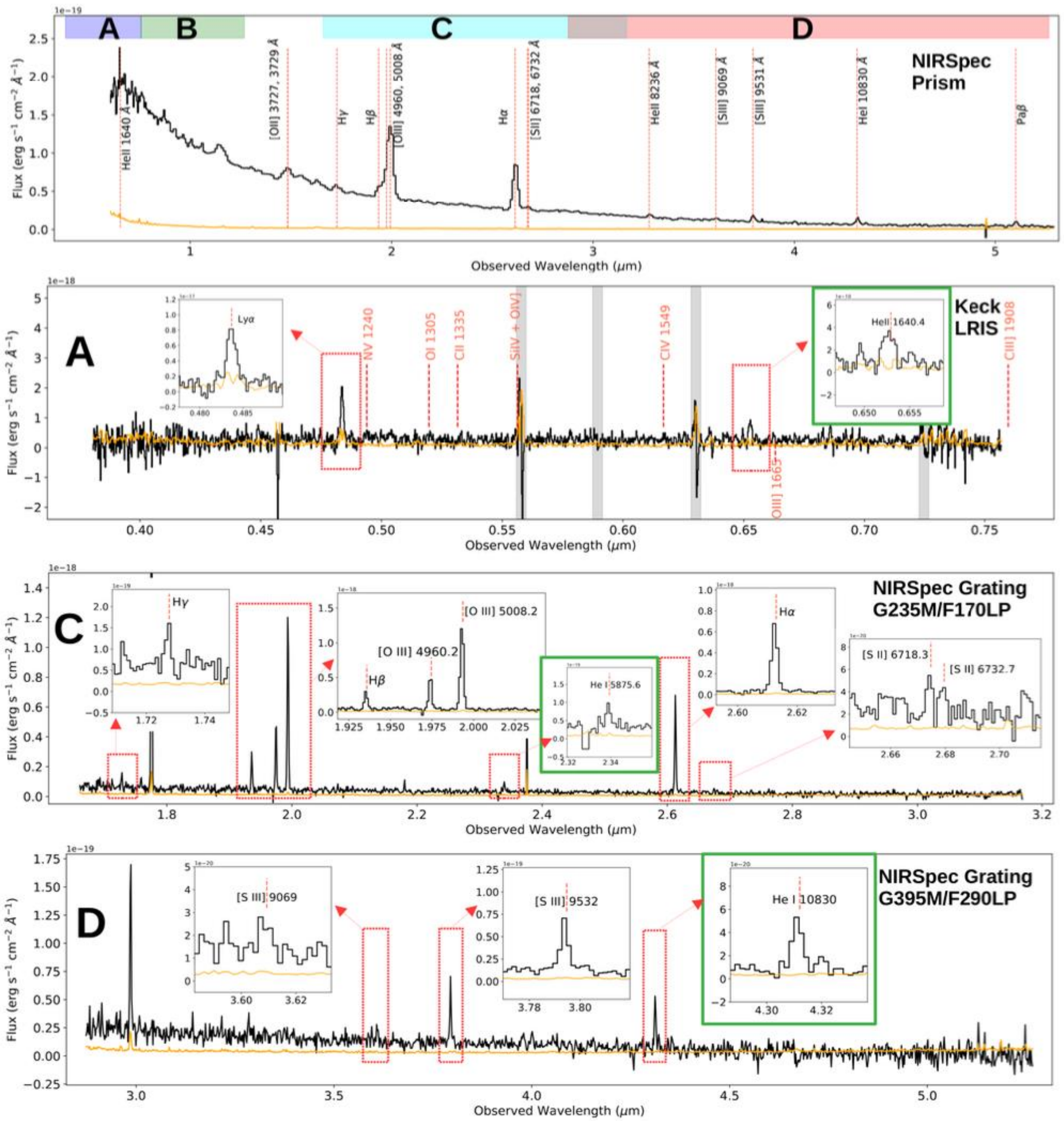

Figure 4. The JWST and Keck spectra that contain all the identified emission lines. In all the panels, the observed spectral fluxes are shown in

Table 4. Derived parameters of the identified emission lines

Emission Line	Wavelength (Å)	Observed flux $\times10^{-18}$ (erg s^{-1}cm^{-2})	Observed FWHM (Å)	FWHM (km s^{-1})	Rest-frame EW (Å)	Instrument
(1)	(2)	(3)	(4)	(5)	(6)	(7)
Lyα	1215.48	23.0±5.4	12.2±1.4	758±90 (690)	19.2	Keck/LRIS
He II λ1640	1640.00	8.8±1.8	12.5±4.2	573±191 (526)	8.3	Keck/LRIS
[OIII] λ4959	4960.1	10.7±2.3	6.5±1.9	99±29 (52)	49.8	Keck/MOSFIRE
[OIII] λ5007	5008.3	59.6±2.2	11.2±0.6	169±10 (146)	248.8	Keck/MOSFIRE
Hγ	4341.5	1.79±0.35	17.1±23.4	296±407*	7.0	NIRSpec G235M/F170LP
Hβ	4863.4	5.44±0.37	20.7±8.9	320±137*	26.6	NIRSpec G235M/F170LP
[OIII] λ4959	4960.8	10.78±0.37	20.3±5.0	308±75*	55.1	NIRSpec G235M/F170LP
[OIII] λ5007	5008.6	29.86±0.52	22.9±1.8	344±26*	155.9	NIRSpec G235M/F170LP
He I λ5875	5877.5	1.60±0.32	23.4±37.0	300±475*	12.2	NIRSpec G235M/F170LP
Hα	6564.7	16.46±0.32	23.4±3.6	268±41*	166.5	NIRSpec G235M/F170LP
[SII] λ6718	6720.0	0.75±0.19	20.1±62.4	225±700*	8.0	NIRSpec G235M/F170LP
[SII] λ6732	6732.3	0.57±0.24	23.5±110.0	263±1241*	6.2	NIRSpec G235M/F170LP
[SIII] λ9069	9068.0	0.61±0.29	46.0±23.4	382±195	11.1	NIRSpec G395M/F290LP
[SIII] λ9532	9533.8	2.10±0.20	34.9±8.9	276±70*	44.8	NIRSpec G395M/F290LP
He I λ10830	10833.4	2.20±0.31	44.7±5.0	311±34	82.1	NIRSpec G395M/F290LP
[OII] λ3727/29	3736±8	3.88±0.01	-	-	13.9	NIRSpec prism
Paβ	12827±3	1.07±0.01	-	-	53.4	NIRSpec prism

* The FWHM values are smaller than the limit of instrumental spectral resolution at that wavelength

Note. Table columns: (1) name of the emission line; (2) rest-frame central wavelength of the line in Å as derived from the fitting; (3) line flux in erg sec^{-1} cm^{-2}; (4) observed FWHM including the fitting error in Å as estimated from the fitted gaussian profile; (5) line FWHM in km s^{-1} - the values in the parenthesis (if any) represents intrinsic FWHM; (6) rest-frame equivalent width of the line in Å ; (7) The instrument used to obtain the corresponding spectrum.